Further Notes on the New Empirical Earthquake Source-Scaling Laws

By Kiran K. S. Thingbaijam and Martin P. Mai

Abstract

We articulate a few additional points, relevant to the empirical earthquake source-scaling laws (Thingbaijam *et al*., 2017). First, we report that adjustments, due to improved theoretical derivation of error-variance ratios, do not impact the general orthogonal regressions significantly. Hence, the earlier results are not affected. Second, we perform partial correlation analysis based on the residuals, to investigate influencing parameter(s) on the scaling relations. It is observed that rupture length L correlates poorly with rupture width W, if not influenced by magnitude M_W. Therefore, overall relation between L and W is controlled by how they scale with M_W independently. On the other hand, average slip correlates negatively with L and more strongly so with W, if influence of M_W is eliminated. Third, we demonstrate that Monte Carlo approach would be appropriate while applying the scaling laws for predictions, to account for the associated data scatter. In case of uncertain independent variable, such approach allows capture the error propagations effectively. Lastly, we evaluate the effect of finite seismogenic depth, in estimation of maximum magnitude for near-vertical strike-slip faults.

Introduction

In this short note, we appraise few points pertinent to the new empirical earthquake source-scaling relations developed by Thingbaijam *et al.* (2017). These include: (1) improved theoretical derivation of error variance ratio applicable for the general orthogonal regressions; (2) correlation analysis of residuals associated with the different relations; (3) prediction of source parameters when the independent variable have measurement error; and (4) impact of finite seismogenic depth on estimation of maximum magnitude M_{max}. These points are relevant to better understanding of the interrelations between the source parameters, and also, to practical applications of the scaling laws.

In the 2017 paper, general orthogonal regression (GOR, Fuller, 1987) was applied to develop the scaling laws. This regression technique accounts for measurement errors of the variables, by using error variance ratio ($\eta = \sigma_y^2/\sigma_x^2$) between the two variables. However, possible correlation between rupture area *A* and average slip *D*, and that between rupture width *W* and rupture length *L* were overlooked in the theoretical derivation of η. Error variance of moment magnitude M_W can be affected by correlation between *A* and *D*, since these two parameters are used to compute the former. Likewise, error variance of *A* would be affected by correlation between *W* and *L*. These factors were not considered previously. Therefore, it would be important to revisit the theoretical derivation of η.

Additionally, we analyze the data scattering associated with the empirical scaling relations. For given three relations such that two of them have a common variable, correlations between residuals (differences between data-points and predicted mean; in order words, data scattering) of these relations can help identify the influencing variable. This approach yields an effective first-order partial correlation analysis. Practically, data scattering is usually considered due to inherent randomness (or aleatoric); for instance, in stochastic rupture scenarios (*e.g.*, Mori *et al.*, 2017). In such cases, multivariate prediction of source parameters can be applied, accounting for correlations between the residuals with different scaling relations (*e.g.*, Goda *et al.*, 2016).

We also address a few issues related to applications of the scaling laws. First, there is concern of possible bias in predicting based on the relations developed using GOR when independent variable has measurement errors (*e.g.*, Das *et al.*, 2018). It would be also important to examine the impact of finite seismogenic depth on estimation of maximum magnitude for near-vertical strike-slip faults. The global scaling relation for strike-slip events exhibits strongly inhibited but unsaturated W with increasing M_W (Thingbaijam *et al.*, 2017). Hence, the global relations would not be applicable if W is saturated due to finite seismogenic depth.

The present study is based on the dataset of source parameters compiled by Thingbaijam *et al.* (2017) and the developed scaling relations. The dataset is based on the rupture models extracted from the SRCMOD database (Mai and Thingbaijam, 2014, see *Data and Resources* section). We do not reproduce the scaling relations here. Typically, they have linear form given by $log_{10}(Y) = bM_W + a$, in which Y can be W, L, A or D. They have been developed, for events

classified into different faulting regimes: shallow crustal reverse-faulting, subduction-interface, strike-slip, and normal-faulting events.

Derivation of Error Variance Ratios

We begin with a brief note on the GOR technique. To obtain the fitting line, it minimizes weighted orthogonal distances from the data-points. The estimate of the slope is given by

$$b = \frac{\sigma_y^2 - \eta\sigma_x^2 + \sqrt{(\sigma_y^2 - \eta\sigma_x^2)^2 + 4\eta\sigma_{xy}^2}}{2\sigma_{xy}} \quad (1)$$

where s_x^2, s_y^2 and s_{xy} are the sample variance of x, variance of y, and covariance between x and y. Then, the intercept is calculated as,

$$a = \bar{y} - b\bar{x} \quad (2)$$

where $\bar{x}$ and $\bar{y}$ are the average of x and y. In case of the source parameters, an appropriate value of η can be theoretically derived from the definition of seismic moment M_0 and M_W.

The definition of seismic moment given by Aki (1966) is

$$M_0 = \mu\, A\, D \quad (3)$$

where μ is crustal rigidity (usually assumed constant and typically μ = 3.3 x 10^{10} Nm^{-2}), and M_W is related to M_0 as follows (Hanks and Kanamori, 1979),

$$M_W = \frac{2}{3} log_{10}(M_0) - 6.03 \quad (4)$$

where M_0 is in Nm. Based on Equations (3) and (4), we can derive the error variance of M_W, in terms of that of $\log_{10}(A)$ and $\log_{10}(D)$. The error variance of M_W be obtained according to Gaussian error propagation, as considered by Thingbaijam *et al.* (2017),

$$\sigma^2_{Mw} = \frac{4}{9} \left(\sigma^2_{log10\,A} + \sigma^2_{log10\,D} \right) \quad (5)$$

This formulation is straight forward. However, if $\log_{10}(A)$ and $\log_{10}(D)$ are correlated then the Gaussian error propagation no longer holds, and the derivation becomes,

$$\sigma^2_{Mw} = \frac{4}{9} \sigma^2_{log10\,A} + \frac{4}{9}\sigma^2_{log10\,D} + \frac{8}{9} cov(log_{10}A, log_{10}D) \quad (6)$$

in which $cov\ (x, y)$ is covariance between x and y where,

$$cov(log_{10}A, log_{10}D) = corr(log_{10}A, log_{10}D)\sigma_{log10A}\sigma_{log10D} \quad (7)$$

where $corr(x, y)$ represents correlation between x and y, in terms of correlation coefficient (for details on propagation of errors, see Kirchner, 2001). Correlation coefficient r provides a

measure such that r = -1 (fully negative correlation), r = 0 (no correlation), and r = 1 (fully positive correlation). In the same manner, the error variance of $\log_{10}(A)$ can be written as,

$$\sigma^2_{log10A} = \sigma^2_{log10\,L} + \sigma^2_{log10\,W} + 2\,cov(log_{10}L, log_{10}W) \quad (8)$$

in which correlation between $\log_{10}(L)$ and $\log_{10}(W)$ is involved.

In most cases, observed correlations $log_{10}(A)$ and $log_{10}(D)$ are poor but positive, with r ranging from 0.29 to 0.43, except for shallow crustal reverse-faulting events for which r ~ 0.72 (Table 2 of Thingbaijam *et al.*, 2017). However, number of events for shallow crustal reverse-faulting events is significantly smaller than other cases. It is possible that variability of stress-drop within the faulting regime has not been well captured, resulting in stronger positive correlation between $log_{10}(A)$ and $log_{10}(D)$. Since these two parameters are non-negative and correlations between these two variables are non-negative as well, we can infer larger uncertainty with M_W, compared to that with $log_{10}(A)$ and $log_{10}(D)$.

Based on Equations 5, 6, 7 and 8, we evaluate the error variance ratios between M_W and $log_{10}(L)$, and between M_W and $\log_{10}(W)$ as follows,

$$\frac{\sigma^2_{log10\,L}}{\sigma^2_{Mw}} \sim \frac{\sigma^2_{log10\,W}}{\sigma^2_{Mw}} \sim \frac{9}{16}\left(\frac{1}{1+corr(log_{10}A, log_{10}D)}\right)\left(\frac{1}{1+corr(log_{10}W, log_{10}L)}\right) \quad (9)$$

such that $corr(log_{10}A, log_{10}D) \geq 0$, and $corr(log_{10}W,\ log_{10}L) \geq 0$. Here, we assume that error variance of $\log_{10}(A)$ and $\log_{10}(D)$ are comparable, following Thingbaijam *et al*. (2017). Likewise, we consider error variance of $log_{10}(L)$ and $log_{10}(W)$ to be in the same order. From Equation 9, we estimate the possible values of $\sigma^2_{log10L}/\sigma^2_{Mw}$ (or $\sigma^2_{log10W}/\sigma^2_{Mw}$) to be in the range from 0.563 to 0.140, for cases of no correlations to that of fully positive correlations between the source parameters.

These variations in the error variance ratios are not significantly large; for example, similar case in Stock and Smith (2000). We find that the estimates of the slope (*b*, in Equation 1), for the relations: M_W–$\log_{10}(W)$ and M_W–$\log_{10}(L)$, increases with decreasing value of error variance ratio. However, these differences in the slope estimates are marginal and not statistically significant. Hence, we conclude that the improved derivation of the error variance ratios do not impact the regressions significantly.

Residual Correlation Analysis

We now investigate the correlations between residuals with the scaling relations. As noted earlier, this analysis measures association between two variables while eliminating influence of a third one. To illustrate, consider three variables: *x*, *y*, and *z* such that linear relationships exist between *x* and y, between x and *z*, and between *y* and *z*. A rational question is whether relationship between *x* and *y* is actual or due to fact that *x* and *y* are independently related to *z*. We evaluate correlation between residuals with regression: $x - z$ and those with regression: $y - z$.

If the correlation is significant, either positive or negative, it implies that relation between *x* and *y* is not controlled by *z*. On the other hand, insignificant correlation would suggest that *x* and *y* are apparently related due to their relationship with *z*. Thus, this analysis will allow new insights into interdependency between the source parameters.

For the overall analysis, number of data-pairs (or events) in the dataset for each faulting types are not adequate for statistical inferences on possible correlations. Therefore, we adopt a bootstrapped approach for the analysis. It involves computation of correlation coefficient repeatedly for 1000 times, each time employing different replacements drawn from the dataset. For the replacements, data-pairs are selected more than once. This approach also allows placing confidence intervals on the estimated correlation coefficient.

Figure 1 summarized the results of the bootstrapped analysis. Here, we examine whether M_W controls the association between the different parameters. We observed that the results are consistent across the different faulting regimes. In case of M_W–$\log_{10}(W)$ and M_W –$\log_{10}(L)$, sample minimums (of computed correlation coefficient) are negative, suggesting that the observed positive correlations could be coincidental. This conclusion is further supported by the computed confidence intervals. This observation implies that *W* and *L* do not have a causal relationship. In a broader sense, this premise agrees with general observed trend of faster growth of *L* with respect to increasing M_W, compared to that of *W* with increasing M_W (*e.g.*, Thingbaijam *et al*., 2017). It also agrees with growth of *L* not restricted by fixed *W* with increasing M_W, a

generally-described and observed feature of *W*-model scaling (*e.g*., Romanowicz and Ruff, 2002).

On the other hand, negative correlations are observed that supports causal associations between $\log_{10}(D)$ and $\log_{10}(L)$ and between with $\log_{10}(D)$ and $\log_{10}(W)$. This observation is intuitive since a smaller A ($= W L$) and larger D can associate M_W similar to that for larger A but with smaller D. In this regard, one can refer to the definition of magnitude (Equations 3 and 4). It also agrees with the hypothesis that D and A are physically related (Thingbaijam and Mai, 2016). Note that this perspective is different from the observed poor but positive correlation between A and D with increasing M_W (discussed in the previous section).

Furthermore, Figure 3 provides a framework for multivariate prediction of the source parameters, taking into account associated uncertainties (aleatoric variability) as well as their interdependencies (*e.g*., Goda *et al*., 2016). This framework supports consideration of L and W, as independent random fields, using $M_W - \log_{10}(L)$ and $M_W - \log_{10}(W)$ relations. On the other hand, aleatoric treatment for D using $M_W - \log_{10}(D)$ relation should incorporate negative correlation between the residuals with M_W–$\log_{10}(A)$ and those with M_W–$\log_{10}(D)$. These constraints would be significant to allow theoretical and observational consistencies in stochastic modeling.

Predicting with the Source-Scaling Relations

In seismic hazard analysis, source-scaling relations are used in different ways. In stochastic modeling of rupture scenarios, a general approach starts with assigning magnitude of the event (*e.g*., Guatteri *et al*., 2004). For a hypothetical event, the magnitude can be based on either seismicity or fault geometry. In case of historical event (documented but not recorded by instruments), the magnitude are usually estimated from macroseismic intensity data, and therefore, can associate significant uncertainty. In case of maximum magnitude, scaling relations are more often used to estimate maximum magnitude associated with identified faults, usually based on measured length of the fault (*e.g*., Mignan *et al*., 2015). In the following, we take up case studies, to address relevant issues.

First, we discuss predictions based on uncertain independent variable. In such cases, regression procedure (applied to develop the scaling relations) would be nontrivial. In earthquake-magnitude conversions, it has been argued that GOR provide actual (true) relations between variables, and may have biased predictions when independent variable has measurement errors (Wason *et al.* 2012; Das *et al*., 2018). To offset this issue, the authors suggested using a modified GOR to develop conversion relations. However, this view has been debated (*e.g*., Gasperini and Lolli, 2013; Gasperini *et al*. 2015). Gasperini *et al*. (2015) reported that GOR line coincides with the data on average, and therefore, modification of GOR is not required.

In case of earthquake-source scaling, actual (average) relations between the source parameter are crucial to allow reliable physical interpretations (*e.g*., Thingbaijam *et al*., 2017). However, it is equally important that the associated data scatter be addressed, for practical applications such as

probabilistic predictions. In this respect, a Monte Carlo approach can be applied to account for the data scatter, to minimize any possible biases from uncertain variable and to avoid complications such as modification of GOR.

To evaluate this approach, we consider two cases of uncertain magnitude for a subduction-interface event: first one defined by a standard deviation: M_W 8.0 (±0.2) with normally-distributed error, and second one given by range: M_W 7.5 to 8.5 with uniformly distributed probability. In each case, we sample M_W independently and obtain the corresponding estimates of $\log_{10}(L)$ and $\log_{10}(W)$. As discussed previously, we consider these two parameters as independent random fields with normally-distributed errors. Figures 2A depicts 100 simulated pairs of $M_W - L$, and $M_W - W$, for the M_W 8.0 (±0.2) event. Figure 2B depicts the same, but for the range of magnitude. Random sampling of these populations can be applied, in situations where fewer scenarios are required.

We note that the mean of these populations coincides with respective scaling relation in all the cases. Also, estimated $\log_{10}(L)$ and $\log_{10}(W)$ are normally-distributed. For a M_W 8.0 event, direct application of scaling relations provide L = 178.7 [139.6, 228.6] in km, and W = 111.7 [88.9, 140.3] in km. The mean estimates are comparable to that obtained from the Monte Carlo simulations: L = 176.0 [124.8, 248.0], and W = 111.5 [86.5, 143.7] for M_W 8.0 (±0.2) and L = 182.5 [111.8, 297.9], and W = 109.5 [77.3, 155.0] for the range: M_W 7.5 to 8.5. However, there are obvious differences in associated standard deviations. The second case exhibits larger variability in the estimated rupture dimensions. Therefore, predictions based on uncertain

independent variable is a problem of error propagation addressable by successive random sampling.

Next, we demonstrate estimation of maximum magnitude M_{max} for long strike-slip fault, traversing hundreds of kilometers. This example is based on the study by Mignan *et al*. (2015) in Anatolian Peninsula, Turkey. The authors provided a comprehensive approach to evaluate multi-segment rupture of strike slip faults. They first evaluated total rupture-length for cascaded ruptures based on geometrical and physical considerations, and then, estimated M_{max} using several scaling relations (from different authors). Here, we compare the different predictions with those from the new scaling relations.

Strike-slip events generally occur on quasi-vertical fault (dip-angles~70°−90°). In such conditions, scaling relations will be affected by physical constraints of finite seismogenic depth. It would be important to note that maximum W for strike-slip events in the global dataset is ~50 *km*, which was reported for an oceanic event − the 2012 M_W~ 8.7 Sumatra earthquake. In this regard, we compare the regressions for global strike-slip events to those for continental strike-slip events. Table 1 lists the scaling coefficients (adopted from Figures 4, 5 and A1, and Table 1 of Thingbaijam *et al.*, 2017). Note that the maximum rupture width in the continental dataset is equal to 32 *km*. In case of L, the scaling coefficients are comparable. On the other hand, the global scaling relation for W tends to predict larger W for larger (M_W >6.5) events and smaller W

for smaller events. However, these differences in the scaling coefficients are not statistically significant if we consider the associated standard errors.

For the continental events, we make an assessment using an independent dataset from Blaser *et al*. (2010). As in Thingbaijam *et al*. (2017), we calculate residuals between this dataset and the scaling relations. Figure 3 shows that the scaling relation for L is consistent with the independent dataset while the median predictions for W tend to be larger (negatively biased). These observations are quite similar to those observed for the global relations.

We reiterate that the relations for global strike-slip events as well as for continental strike-slip events do not exhibit saturation of W. Therefore, region-specific studies, where finite seismogenic depth (< 50 km) is established; $M_W - \log_{10}(A)$ scaling should be preferred, and thereby, adjusting the scaling of L with respect to M_W. Note that the scaling of A with respect to M_W is assumed to be unaffected by dynamics of finite seismogenic depth (Leonard, 2010; Thingbaijam e*t al*., 2017). Accordingly, we consider maximum seismogenic depth of 18 km for the present analysis, as adopted by Mignan *et al*. (2015). This consideration deviates the scaling of L from global scaling (consistent with L-model) to that more aligned with W-model scaling. The L- and W-models have been widely discussed in literature (Scholz, 1982; Romanowicz, 1992).

In Figure 4, the adjusted $\log_{10}(L) - M_W$ scaling predict similar magnitudes at L >100 km, with those given by Anderson *et al*. (1996), Wesnousky (2008), and Leonard (2010). These scaling

relations were preferred by previous studies (Mignan *et al.*, 2015; Leonard, 2015). For comparison, we also include that of Hanks and Bakun (2002), which closes to that of Thingbaijam *et al.* (2017) with increasing L.

In Anatolian Peninsula, Mignan *et al.* (2015) calculated two possible maximum rupture length L_{max} = 853 km, and =1480 km. For these L_{max} values, we obtain M_{max} equal to M_W 8.15 (±0.18) and M_W 8.40 (±0.18). These M_{max} estimates are close to that previously predicted by Mignan *et al.* (2015) and Leonard (2015), whose mean values lies between M_W 8.11 and M_W 8.30 for the first case, and between M_W 8.32 to 8.53 for the second one. Thus, the global relations can be easily adjusted according to region-specific finite seismogenic depth. However, uncertainty with finite seismogenic depth has not been considered in the present example. Higher seismogenic depth (and consequently larger maximum W) will increase the estimated M_{max}, and thereby, potentially increase the calculated seismic hazard.

Conclusions

We conclude with the following remarks. First, it is appropriate to consider correlation between A and D and that between L and W, in the theoretical derivation of error variance ratio between the source parameters. However, this improvement over the previous derivation by Thingbaijam *et al.* (2017) does not affect the results of general orthogonal regressions significantly. Therefore, the developed scaling relations remain applicable. Second, partial correlation analysis of the

residuals suggests that L is poorly correlated with W, for a given M_W. However, D correlates strongly and negatively with L and with W, if not influenced by M_W. Third, Monte Carlo simulations allow appropriate use of the scaling laws for predictions incorporating the associated data scatter. In case of uncertain independent variable, this approach can be applied, to account for the error propagations effectively. Lastly, $M_W - log_{10}(A)$ scaling is preferred and provide realistic prediction of M_{Max}, in case of saturated growth of W due to finite seismogenic depth.

Data and Resources

The SRCMOD database can be accessed online at http://equake-rc.info/srcmod/ (last accessed, August 2018). The catalogue of source parameters estimated by Thingbaijam *et al*. (2017) is available in their electronic supplement. Likewise, the dataset of Blaser *et al.* (2010) is available in their electronic supplement.

Acknowledgements

The research presented in this article is supported by King Abdullah University of Science and Technology (KAUST) in Thuwal, Saudi Arabia.

References

Aki, K. (1966). Generation and propagation of G waves from the Niigata earthquake of June 16, 1964: Part 2. Estimation of earthquake moment, released energy and stress drop from the G wave spectra, *Bull. Earthq. Res. Inst., Univ. Tokyo* **44**, 73–88.

Anderson, J. G., S. G. Wesnousky, and M. W. Stirling (1996). Earthquake size as a function of fault slip rate, *Bull. Seismol. Soc. Am.* **86**, 683–690.

Blaser, L., F. Krüger, M. Ohrnberger, and F. Scherbaum (2010). Scaling relations of earthquake source parameter estimates with special focus on subduction environment, *Bull. Seismol. Soc. Am.* **100**, 2914–2926.

Castellaro, S., F. Mulargia, and Y.Y Kagan (2006). Regression problems for magnitudes, *Geophys. J. Int.* **165**, 913–930.

Das, R., H. R. Wason, G. Gonzalez, M. L. Sharma, D. Choudhury, C. Lindholm, N. Roy, and P. Salazar (2018). Earthquake magnitude conversion problem, *Bull. Seismol. Soc. Am.* **108**, 1995–2007.

Fuller, W. A. (1987). *Measurement error models.* John Wiley & Sons, New York

Gasperini, P. and B. Lolli (2013). Comment on 'Magnitude conversion problem using general orthogonal regression' by HR Wason, Ranjit Das and ML Sharma, (Geophys. J. Int., 190, 1091–1096), *Geophys. J. Int.* **196**, 626–627.

Gasperini, P., B. Lolli, and S. Castellaro (2015). Comparative analysis of regression methods used for seismic magnitude conversions, *Bull. Seismol. Soc. Am.* **105**, 1787–1791.

Guatteri, M., P.M. Mai, and G.C. Beroza (2004). A pseudo-dynamic approximation to dynamic rupture models for strong ground motion prediction, *Bull. Seismol. Soc. Am.* **94**, 2051–2063.

Goda, K., T. Yasuda, N. Mori, and T. Maruyama (2016). New scaling relationships of earthquake source parameters for stochastic tsunami simulation, *Coast. Eng. Jour.* **58**, doi: http://dx.doi.org/10.1142/S0578563416500108

Hanks, T. C., and W. H. Bakun (2002). A bilinear source-scaling model for M − log A observations of continental earthquakes, *Bull. Seismol. Soc. Am.* **92**, 1841–1846.

Hanks, T. C., and H. Kanamori (1979). A moment magnitude scale, *J. Geophys. Res*. **84**(B5), 2348–2350, doi:10.1029/JB084iB05p02348.

Kirchner, J. (2001). Data analysis toolkit #5—Uncertainty analysis and error propagation: Analysis of Environmental Data Course, University of California, Berkely, California, USA

Leonard, M. (2010). Earthquake fault scaling: relating rupture length, width, average displacement, and moment release. *Bull. Seismol. Soc. Am*. **100**, 1971–1988.

Leonard, M. (2015). Comment on "Reassessment of the Maximum Fault Rupture Length of Strike-Slip Earthquakes and Inference on M max in the Anatolian Peninsula, Turkey" by A. Mignan, L. Danciu, and D. Giardini. *Seismol. Res. Lett*.**86**, 1690–1691.

Mai, P. M., and K. K. S. Thingbaijam (2014). SRCMOD: an online database of finite-fault rupture models. *Seism. Res. Lett.* **85**, 1348–1357.

Mignan, A., L. Danciu, and D. Giardini (2015). Reassessment of the maximum fault rupture length of strike-slip earthquakes and inference on Mmax in the Anatolian peninsula, Turkey, *Seismol. Res. Lett*.**86**, 890–900.

Mori, N., P.M. Mai, K, Goda, and T. Yasuda (2017). Tsunami inundation variability from stochastic rupture scenarios: Application to multiple inversions of the 2011 Tohoku, Japan earthquake. *Coastal Engineering* **127**, 88–105.

Romanowicz, B. (1992). Strike-slip earthquakes on quasi-vertical transcurrent faults: Inferences for general scaling relations, *Geophys. Res. Lett*. **19**, 481–484.

Scholz, C. H. (1982). Scaling laws for large earthquakes: consequences for physical models, *Bull. Seismol. Soc. Am.* **72**, 1–14.

Stock, C. and S.G. Smith (2000). Evidence for different scaling of earthquake source parameters for large earthquakes depending on faulting mechanism. *Geophys. Jour. Int.* **143**, 157–162.

Thingbaijam, K. K. S., and P. M. Mai (2016). Evidence for truncated exponential probability distribution of earthquake slip, *Bull. Seismol. Soc. Am.* **106**, 1802–1816.

Thingbaijam, K.K.S., P. M. Mai, and K. Goda (2017). New empirical earthquake source-scaling laws, *Bull. Seismol. Soc. Am.* **107**, 2225–2246.

Wason, H.R., R. Das and M.L. Sharma (2012). Magnitude conversion problem using general orthogonal regression, *Geophys. J. Int.* **190**, 1091–1096.

Wesnousky, S. G. (2008). Displacement and geometrical characteristics of earthquake surface ruptures: Issues and implications for seismic-hazard analysis and the process of earthquake rupture, *Bull. Seismol. Soc. Am.* **98**, 1609–1632.

Kiran Kumar S. Thingbaijam

Martin P. Mai

Physical Science and Engineering Division

King Abdullah University of Science & Technology

Thuwal 23955-6900, Saudi Arabia

k.thingbaijam@kaust.edu.sa

martin.martin@kaust.edu.sa

TABLE

Table 1

Scaling Coefficients between Rupture Length, Rupture Width, and Moment Magnitude

Faulting Regime	**Equation**	***b* (*sb*)**	***a* (*sa*)**	***σ***	***r***	**Data range**	
						M_W	**Dimension**
Continental Strike-slip	$\log_{10} L = a + b\, M_W$	0.674 (0.061)	-2.905 (0.420)	0.156	0.84	5.38 – 7.91	6.0 – 330 km
	$\log_{10} W = a + b\, M_W$	0.210 (0.028)	-0.233 (0.192)	0.093	0.68	5.38 – 7.91	6.5 – 32.0 km
Global strike-slip	$\log_{10} L = a + b\, M_W$	0.681 (0.052)	-2.943 (0.357)	0.151	0.88	5.38 – 8.70	6.0 – 580.0 km
	$\log_{10} W = a + b\, M_W$	0.261 (0.026)	-0.543 (0.179)	0.105	0.75	5.38 – 8.70	6.5 – 50.0 km

- The notations in the Equations: L, W and M_W denote rupture length, rupture width, and moment magnitude. The slope and intercept are given by b and a, and their standard errors by *sb* and *sa*, while the stand deviation is given by σ. The correlation coefficient is denoted by *r*.

FIGURES

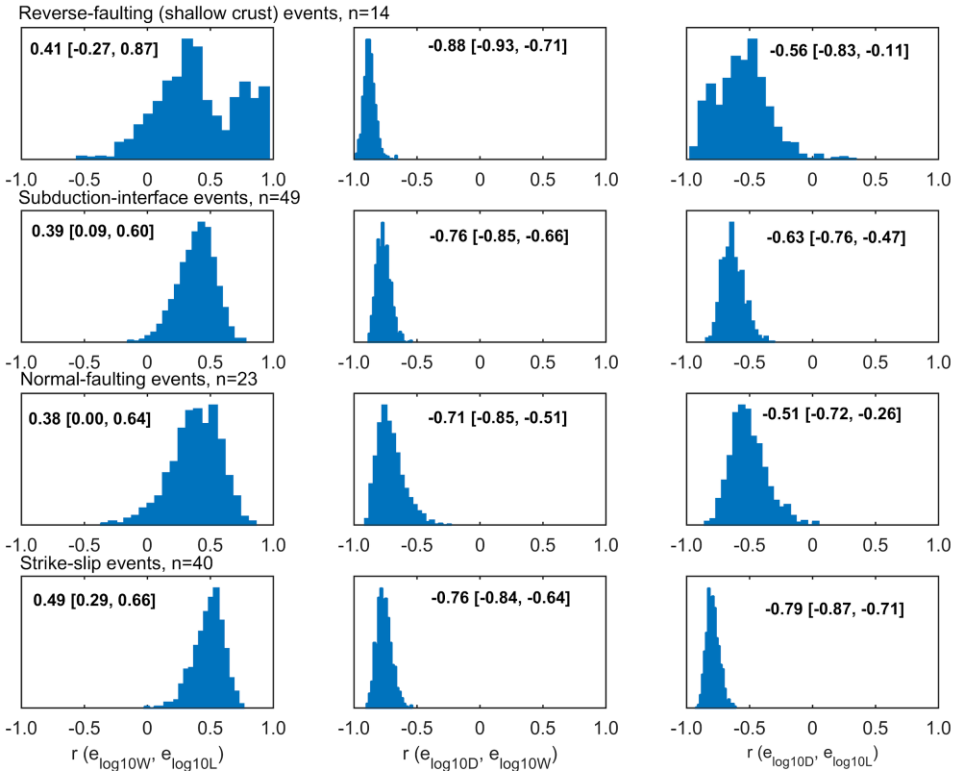

Figure 1. Distributions of correlation coefficient *r* given by bootstrapped correlation analysis of residuals: each row shows a set of analysis for the faulting regime (as indicated) with the total number of events in the original dataset given by *n*. The residuals are denoted by *e* for scaling relation of a source parameter indicated in subscript, for instance e_{log10W} stands for residuals associated with $M_W - \log_{10}(W)$ relation. *W*, *L*, and *D* stands rupture width, rupture length and average slip. Mean and confidence interval (in square brackets) for estimated *r* are annotated on each plot. Overall, $\log_{10}(W)$ and $\log_{10}(L)$ have poor correlation while $\log_{10}(D)$ have strong negative correlation with $\log_{10}(W)$ as well as with $\log_{10}(L)$, if influences of magnitude M_W is eliminated.

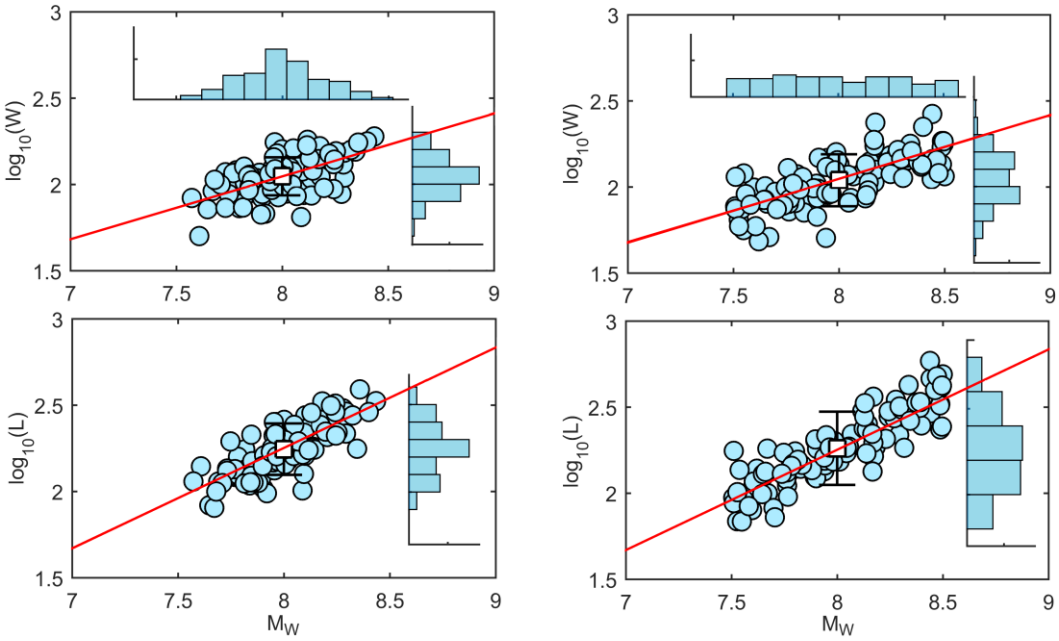

Figure 2. Monte Carlo realizations of uncertain magnitude and the corresponding rupture length *L* and rupture width *W*, for a subduction-interface event, estimated 100 times using the scaling relations (depicted by the solid lines): (A) M_W 8.0 with normally-distributed error with standard deviation equal to ±0.2, and (B) uniformly-distributed magnitude in range: M_W 7.5−8.5. In both the cases, estimated log_{10} (*L*) and log_{10} (*W*) are normally distributed; mean and standard deviation is indicated by box and error bar.

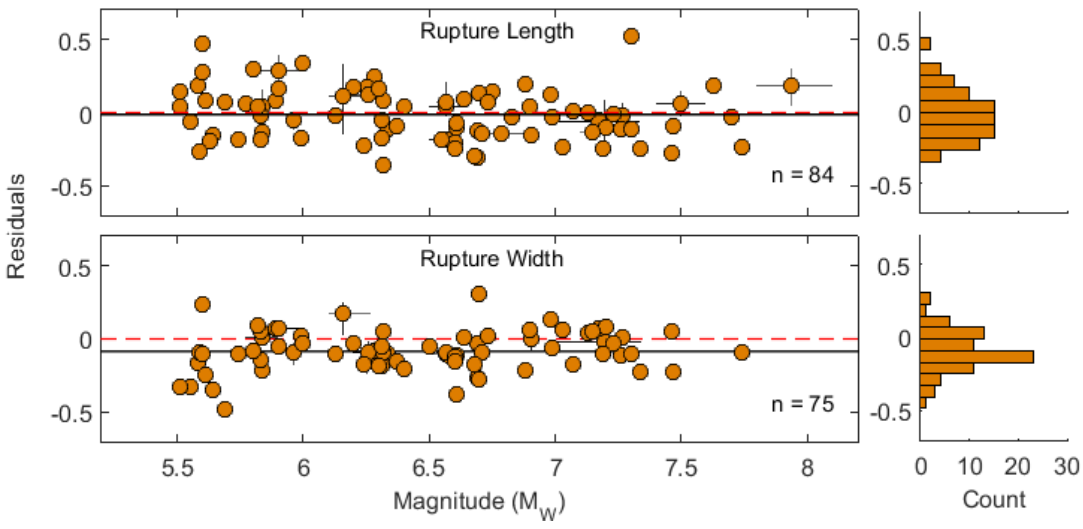

Figure 3. An assessment of the empirical scaling of continental strike-slip earthquakes using independent dataset from Blaser *et al*. (2010) is given by distribution of the residuals (difference between actual and predicted value on $\log_{10}$ scale). The actual values are from the independent dataset, and predicted values are obtained by applying the empirical scaling relations.

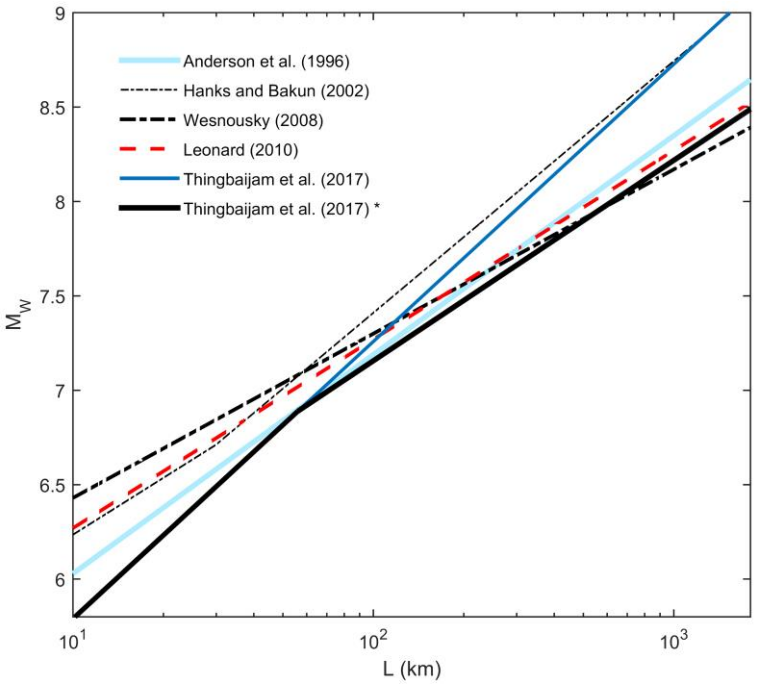

Figure 4. The plot depicts scaling of magnitude M_W with respect to rupture length L for strike-slip earthquakes given by different empirical scaling relations. At L >100 km, Anderson *et al*. (1996), Wesnousky (2008), Leonard (2010) and Thingbaijam *et al*. (2017)* clusters while Hanks and Bakun (2002) is closer to Thingbaijam *et al*. (2017). The asterisk indicated that estimated M_W is based on rupture area, instead of L accounting for finite seismogenic depth ~18 *km*.